SCIENCE CHINA
Life Sciences

• RESEARCH PAPER •

September 2014 Vol.57 No.9: 915–924
doi: 10.1007/s11427-014-4687-1

Overexpression of a dominant-negative mutant of SIRT1 in mouse heart causes cardiomyocyte apoptosis and early-onset heart failure

MU WenLi, ZHANG QingJun, TANG XiaoQiang, FU WenYan, ZHENG Wei, LU YunBiao, LI HongLiang, WEI YuSheng, LI Li, SHE ZhiGang, CHEN HouZao* & LIU DePei*

State Key Laboratory of Medical Molecular Biology, Department of Biochemistry and Molecular Biology, Institute of Basic Medical Sciences, Chinese Academy of Medical Sciences & Peking Union Medical College, Beijing 100005, China

Received March 31, 2014; accepted April 30, 2014; published online August 6, 2014

SIRT1, a mammalian ortholog of yeast silent information regulator 2 (Sir2), is an NAD^+-dependent protein deacetylase that plays a critical role in the regulation of vascular function. The current study aims to investigate the functional significance of deacetylase activity of SIRT1 in heart. Here we show that the early postnatal hearts expressed the highest level of SIRT1 deacetylase activity compared to adult and aged hearts. We generated transgenic mice with cardiac-specific expression of a dominant-negative form of the human SIRT1 (SIRT1H363Y), which represses endogenous SIRT1 activity. The transgenic mice displayed dilated atrial and ventricular chambers, and died early in the postnatal period. Pathological, echocardiographic and molecular phenotype confirmed the presence of dilated cardiomyopathy. Terminal deoxynucleotidyl transferase-mediated dUTP nick-end-labeling analysis revealed a greater abundance of apoptotic nuclei in the hearts of transgenic mice. Furthermore, we show that cardiomyocyte apoptosis caused by suppression of SIRT1 activity is, at least in part, due to increased p53 acetylation and upregulated Bax expression. These results indicate that dominant negative form of SIRT1 (SIRT1H363Y) overexpression in mouse hearts causes cardiomyocyte apoptosis and early-onset heart failure, suggesting a critical role of SIRT1 in preserving normal cardiac development during the early postnatal period.

deacetylase, SIRT1, apoptosis, heart failure

Citation: Mu WL, Zhang QJ, Tang XQ, Fu WY, Zheng W, Lu YB, Li HL, Wei YS, Li L, She ZG, Chen HZ, Liu DP. Overexpression of a dominant-negative mutant of SIRT1 in mouse heart causes cardiomyocyte apoptosis and early-onset heart failure. Sci China Life Sci, 2014, 57: 915−924, doi: 10.1007/s11427-014-4687-1

SIRT1, a mammalian ortholog of yeast silent information regulator 2 (Sir2), is an NAD^+-dependent histone and protein deacetylase and belongs to the class III HDAC family [1]. SIRT1 contains a highly conserved catalytic domain [1,2], and a point mutation in the catalytic domain effectively abolishes the deacetylase activity [3,4]. The deacetylating substrates of SIRT1 include histones, a variety of important transcription factors and some transcription co-factors [5]. Most studies characterize that SIRT1 protects against aging-associated diseases including cardiovascular diseases, metabolic disorders, cancer and neurodegenerative disease [6]. SIRT1 is also crucial for improving metabolism and health span [7–9].

In embryo, SIRT1 expresses mainly in the heart and brain [10]. General knockout study shows that SIRT1 plays a role in heart development and morphogenesis, but there are a small percentage of mice survive to adulthood without showing heart structural abnormalities [11]. SIRT1 is highly expressed in the vasculature [12] and is atheroprotective in endothelial cells [13,14], smooth muscle cells [15] and macrophages [16]. SIRT1 has also been shown to protect hyperglycemia-induced endothelial dysfunction [17], and prevent vascular neointima formation [18]. In the heart, SIRT1 has been shown to act as an important survival factor

*Corresponding author (email: liudp@pumc.edu.cn; houzao@gmail.com)

for cardiomyocytes during stress [19–21]. Mild overexpression of SIRT1 in the heart protects oxidative stress-induced cardiac ageing and retards age-dependent cardiac dysfunction, while high levels of SIRT1 expression induces oxidative stress and cardiomyopathy [22]. In addition, SIRT1 has the characteristics of prevention of cardiac hypertrophy [22,23], but it was also shown to promote cardiac hypertrophy and heart failure together with PPARα [24]. Furthermore, SIRT1 participates essentially in protecting hearts from ischemia-reperfusion injury [25–27]. Several studies from our laboratory and others indicate that SIRT1 deacetylase activity plays a critical role in the regulation of vascular function [12,28–31], however, the role of deacetylase activity of SIRT1 in the heart is not fully investigated.

In the present study, we demonstrate that the early postnatal hearts express the highest level of SIRT1 deacetylase activity. Then we generated transgenic mice that exhibit cardiac-specific expression of a dominant-negative form of the human SIRT1 (SIRT1H363Y), which resulted in a significant decrease in SIRT1 deacetylase activity in the hearts. SIRT1H363Y overexpression in mouse hearts increased cardiomyocyte apoptosis and caused severe dilated cardiomyopathy, leading to deterioration of cardiac function and early death during the postnatal period.

1 Materials and methods

1.1 Assessment of SIRT1 deacetylase activity

SIRT1 deacetylase activity was determined using the SIRT1 Fluorimetric Kit (Biomol International, LP, Plymouth Meeting, PA, USA), according to the manufacturer's instructions as previously described [32]. Briefly, crude nuclear extract samples prepared from FVB/N mice at postnatal age of 7 d, 2, 18 and 24 months, TG mice or WT littermates on postnatal day 4 (P4) (10 μg protein/well) were incubated in 40 mmol L^{-1} Tris-HCl (pH 7.4) containing 500 μmol L^{-1} NAD, and 100 μmol L^{-1} Fluor de Lys-SIRT1 substrate at 37°C for 1 h. Following incubation, the reaction was terminated by the addition of a solution containing Fluor de Lys Developer and 2 mmol L^{-1} nicotinamide. Values were determined by reading fluorescence on a fluorimetric plate reader (Spectramax Gemini XPS, Molecular Devices, Sunnyvale, CA, USA) with an excitation wavelength of 360 nm and emission wavelength of 460 nm.

1.2 Generation of α-MHC-SIRT1H363Y transgenic mouse

All of the animal protocols were approved by the Animal Care and Use Committee at the Institute of Basic Medical Sciences, Chinese Academy of Medical Sciences and Peking Union Medical College. Full length cDNA encoding SIRT1H363Y was a generous gift of Prof. Fuyuki Ishikawa [33]. To establish transgenic mouse lines with cardiac-specific expression, the DNA fragment corresponding to the full-length coding region of SIRT1H363Y was sub-cloned into the blunted *Sal*I site of a plasmid containing the full-length (5.5 kb) murine α-MHC promoter [34]. Fragments containing the transgenic construct and the pronuclear stage zygotes of FVB/N mice were used for microinjection. In all experiments, transgenic founders were identified and bred to produce offspring for analysis, and age-matched wild-type (WT) littermates were used for comparison with the SIRT1H363Y transgenic (TG) mice. Mice were anesthetized by intraperitoneal injection of Avertin (400 mg kg^{-1}) (Sigma-Aldrich, St. Louis, USA) and were euthanized by cervical dislocation prior to tissue collection.

1.3 Echocardiography

Echocardiography was performed as previously described [35]. Two-dimensional short-axis images were obtained using a high resolution Vevo 770 Imaging System (Visualsonics Inc., Toronto, Canada) equipped with a 35 MHz probe. Left ventricular chamber dimension and wall thickness during systolic and diastolic phases were measured from the M-mode images. Left ventricular volume, fractional shortening (FS) and ejection fraction (EF) were calculated using the Vevo Analysis program. Body temperature was kept constant with a heating pad.

1.4 Histological analysis and immunohistochemistry

Histological analysis and immunohistochemistry were performed as previously described [36]. Sections (5 μm) were stained with hematoxylin & eosin (H&E) and picrosirius red for histopathological analyses. Quantitative assessment of the fibrotic area of the myocardium was performed on five sections in five randomly selected fields per section by quantitative morphometry of left ventricular tissue sections. Paraffin-embedded sections were incubated with anti-SIRT1 antibody (1:100, Santa Cruz Biotechnology Inc., Santa Cruz, USA) followed by biotin-streptavidin horseradish peroxidase (HRP) kit (Vector Laboratory, CA, USA).

1.5 Evaluation of apoptosis in tissue sections and cardiomyocytes

DNA fragmentation was detected *in situ* using terminal deoxynucleotidyl transferase-mediated dUTP nick-end labeling (TUNEL), as previously described [21]. Briefly, paraffin-embedded sections were evaluated for apoptosis by means of TUNEL (DeadEnd Fluorometric TUNEL System, Promega, Madison, USA) according to the manufacturer's protocol. Percentage of apoptosis was determined by the number of TUNEL positive myocytes divided by that of Hoechst-positive nuclei in six separate fields.

1.6 Primary culture of neonatal rat ventricular myocytes

Neonatal rat ventricular myocytes from 1 to 3-day-old Sprague-Dawley rats were prepared as previously described [37]. Myocytes were cultured under serum-free conditions for 48 h before experiments. SIRT1 inhibitor Sirtinol was purchased from Sigma and the Bax-inhibitory peptide V5 and negative control peptide were purchased from Calbiochem (Marmstadt, Germany).

1.7 Western blot analysis

Western blotting was performed as previously described [21] with the following antibodies: anti-SIRT1, anti-Bcl-2, anti-Bcl-XL, anti-Bax, anti-GAPDH (Santa Cruz Biotechnology Inc., Santa Cruz, USA); anti-cleaved-caspase-3 (Asp175), anti-c-FLIP, anti-caspase-8, anti-caspase-9 (Cell Signaling, Beverly, USA); anti-acetylated-p53 (Lys373, Lys382) (Upstate, New York, USA); anti-Apaf-1 (CellChip, Beijing, China); anti-β-Actin (Sigma, St. Louis, USA). Briefly, mouse hearts were homogenized in a buffer (150 mmol L^{-1} NaCl, 5 mmol L^{-1} EDTA, 1% Tween-20, 50 mmol L^{-1} Tris, pH 7.4, protease inhibitor cocktail (Sigma, St. Louis, USA)), incubated on ice for 30 min, sonicated, then centrifuged at 25000×*g* for 1 h. Pellets were suspended in high-ionic strength buffer (1.5 mol L^{-1} KCl rather than 50 mmol L^{-1} NaCl) to extract insoluble fractions.

1.8 Polymerase chain reaction (PCR) assay

RNA was extracted by TRIzol (Invitrogen, Carlsbad CA, USA). Two μg of total RNA was reverse transcribed with M-MuLV transcriptase (New England BioLabs, Massachusetts, USA) according to the manufacture's protocol. The cDNAs were subjected to either conventional reverse transcription PCR (SIRT1, ANP, BNP) or real-time PCR (Bax, Noxa, Puma and GAPDH) with SYBR Green methods. Primers are provided in Table S1 in Supporting Information. The mean expression level of each gene was normalized to that of GAPDH.

1.9 Statistic analysis

Results are expressed as mean±SEM. Differences between the two groups were determined by a Student's *t* test. Differences were considered significant at a value of $P<0.05$.

2 Results

2.1 SIRT1 deacetylase activity is high in early postnatal hearts

We first examined SIRT1 deacetylase activity in postnatal hearts. Crude nuclear extract samples were prepared from the hearts on postnatal day 7 (7D), and from the hearts of 2-month-old (2M), 18-month-old (18M) and 24-month-old (24M) mice. The postnatal day 7 hearts expressed the highest level of SIRT1 deacetylase activity (Figure 1), which was approximately 4-fold higher than the 2-month hearts did. The SIRT1 deacetylase activity in 18-month and 24-month hearts was only about 10% of that on postnatal day 7 (Figure 1). These results suggest that SIRT1 deacetylase activity may play an important role in the early postnatal hearts.

2.2 Characterization of SIRT1H363Y transgenic mice

We next generated transgenic (TG) mice that expressed SIRT1H363Y driven by the cardiac-specific α-MHC promoter (Figure 2A) to investigate the requirement for SIRT1 deacetylase activity in the postnatal ventricular myocardium *in vivo*. This mutant SIRT1 protein has been shown to function as a potent dominant-negative inhibitor of SIRT1-dependent deacetylase activity [4]. Unexpectedly, most of the TG founder mice exhibited overt signs of heart failure, including shortness of breath and peripheral edema. These mice abated physical activity a few days before death and died from one week to four weeks after birth. Fortunately, three lines of TG founder mice (Nos. 4, 30 and 50) survived (Figure 2B). A robust expression of SIRT1H363Y protein was found in the heart (Figure 2C). No significantly phenotypic difference was observed among these three established lines of TG mice. TG4# mice expressed the highest level of the SIRT1H363Y protein (Figure 2B), in which cardiac SIRT1H363Y expression was also identified by immunohistochemistry (Figure 2D), and the offspring of TG4# were used for further experiments unless specially indicated. To test whether SIRT1 deacetylase activity could be inhibited by SIRT1H363Y overexpression, SIRT1 deacetylase activity was determined. TG mouse hearts overexpressing SIRT1H363Y had a 65 percent decrease in SIRT1 deacety-

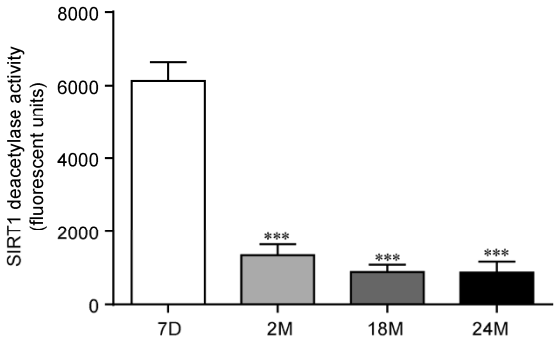

Figure 1 SIRT1 deacetylase activity in mouse hearts at different stages of postnatal life. SIRT1 deacetylase activity in the neonatal hearts from postnatal day 7 (7D), and adult hearts from 2 months (2M), 18 months (18M) and 24 months (24M) were examined. Extract nuclear samples were prepared at the indicated time points. SIRT1 deacetylase activity was determined by reading fluorescence on a fluorimetric plate reader as described under "Materials and methods". Values are expressed as mean±SEM (n=5). ***, $P<0.001$ vs. sample from 7D.

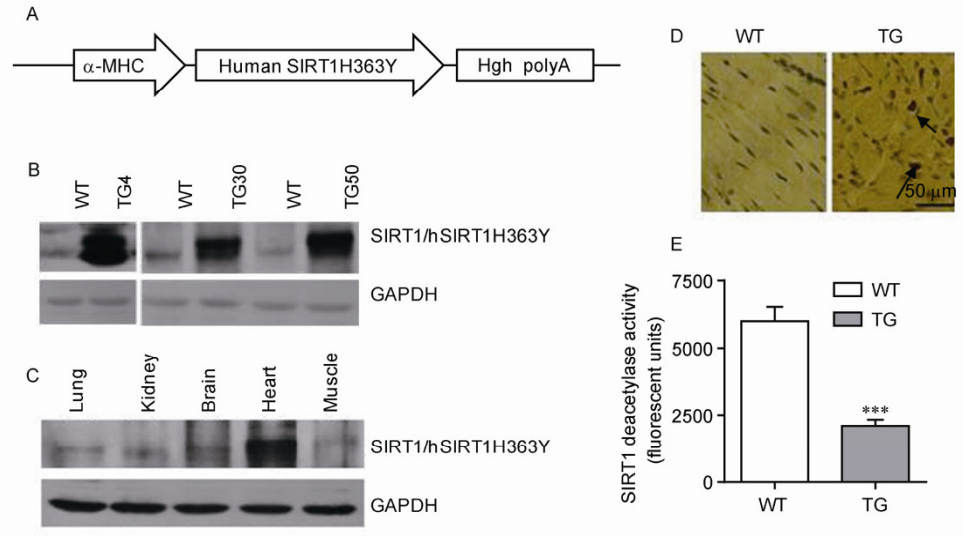

Figure 2 Characterization of SIRT1H363Y TG mice. A, Diagram of the transgene construct used for the generation of SIRT1H363Y TG mice. The construct contains the α-MHC promoter, the full-length human SIRT1H363Y (hSIRT1H363Y) clone and a human growth hormone poly adenylylation. B, Representative Western blot analysis of hSIRT1H363Y protein in the heart tissue from 3 lines of TG mice and WT littermates. C, Representative Western blot analysis of hSIRT1H363Y protein from different organs of TG mice. D, Immunohistochemical staining for hSIRT1H363Y expression of the left ventricles of TG mice and WT littermates. The result shows a large increase in expression of hSIRT1H363Y in TG mouse hearts. Positive-stained cells appear brown. Scale bar, 50 μm. E, Deacetylase activity was evaluated for 1 h with a fluorometric assay of crude nuclear extracts from 4D old TG mouse hearts and WT littermates (n=5). Values are expressed as mean±SEM. ***, P<0.001 vs. WT.

lase activity compared with wild-type (WT) littermates (Figure 2E). The fact that the dominant-negative effects of SIRT1H363Y protein are mostly lethal supports a crucial role for SIRT1 deacetylase activity in cardiomyocytes during postnatal life.

2.3 SIRT1H363Y transgenic mice develop dilated cardiomyopathy and heart failure

At birth, SIRT1H363Y TG pups were indistinguishable from WT littermates. Unexpectedly, they became weak and inactive a few days after birth and died mainly from postnatal days 8 to 12 (Figure 3A). We analyzed the ratio of heart weight to body weight (HW/BW) in surviving animals at postnatal days 4, 6, 8 and 10, and found that the HW/BW ratio of TG mice was significantly greater than that of WT controls at postnatal days 8 and 10 (Figure 3B), indicating an enlargement of TG mouse hearts. TG founder mouse 50# died suddenly at 8 months of age. Necropsy showed enlargement of both atria and ventricles, with a large organized thrombus in the left atrium (Figure S1A and B in Supporting Information), indicative of chronic heart failure. Using echocardiography, we discovered that left ventricular internal dimensions (LVID) were markedly raised in TG mouse hearts compared to WT littermates at P7. In addition, left ventricular anterior wall (LVAW) and left ventricular posterior wall (LVPW) of TG mice were markedly thinner than that in controls (Figure 3C, Table 1). These results suggest that the TG mice showed a phenotype of dilated cardiomyopathy. Functional assessment revealed significant augment in both diastolic and systolic ventricular chamber volumes, associated with abnormal cardiac function in TG mice, including a remarkable reduction in fractional shortening (FS) and ejection fraction (EF). The overall results of echocardiography are summarized in Table 1. We compared the left ventricular internal diastolic dimension (LVIDd) and the EF of TG mouse hearts with WT controls over five days of continuous observations. In TG mice, the left ventricle became dilated, with an LVIDd of 2.3±0.19 mm, versus 1.64±0.04 mm in WT controls on postnatal day 6 (Figure 3D). In addition, systolic function of the TG mouse hearts was gradually declined, with an EF decreased to 58%±4%, versus 93.3%±4.2% in WT controls on postnatal day 6 (Figure 3E). We further examined the mRNA level of atrial natriuretic peptide (ANP) and brain natriuretic peptide (BNP), two markers of molecular phenotype of heart failure. The results showed that ANP and BNP were up-regulated in TG mouse hearts (Figure 3F). These above data suggest that TG mice express the features of dilated cardiomyopathy including an early defect in contractility and rapid progression towards overt heart failure.

To further assess alterations in the cardiac structure of these TG mice, we performed histological analyses. Both the atria and ventricles of TG mice displayed substantial dilatation (Figure 4A and B). Histological examination revealed marked heterogeneity in cardiomyocyte size in TG mouse hearts, relative to WT controls (Figure 4C). However, no significant difference in cross-sectional area was observed between WT and TG groups (Figure 4D). Picrosirius red staining also revealed an increased level of interstitial

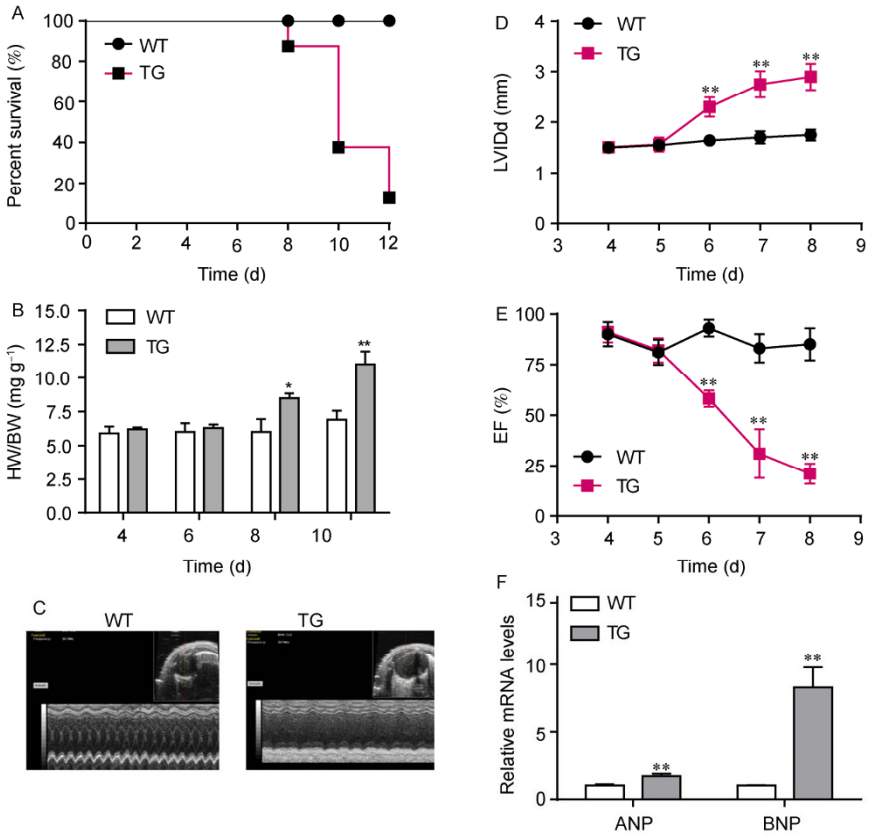

Figure 3 (color online) SIRT1H363Y transgenic mice developed dilated cardiomyopathy and heart failure. A, Survival curve of TG mice. The F_1 generation of TG mice died mainly from postnatal day 6 to 12. Most of TG mice died at postnatal day 14 (n=24), but all WT littermates survived (n=20). B, Heart weight (mg) to body weight (g) ratio (HW/BW) in TG mice and WT littermates at various days. The HW/BW ratio increased in TG mice compared with WT littermates at postnatal days 8 and 10. Values are expressed as mean±SEM (n=6). *, P<0.05; **, P<0.01 vs. WT. C, Echocardiograph analysis of TG mice and WT littermates at various days. Left ventricular internal diastolic dimension (LVIDd) (D) and ejection fraction (EF) (E) were measured by echocardiography on conscious animals at postnatal day 4 to 8. Values are expressed as mean±SEM (n=6). **, P<0.01. F, Elevated heart failure marker gene expression in TG mouse hearts. ANP and BNP expression of TG mouse hearts and WT littermates of P7 were analyzed by PCR with specific primers. Values are expressed as mean±SEM (n=4). **, P<0.01 vs. WT.

Table 1 Echocardiograph analysis of hSIRT1H363Y TG and WT mice[a)]

	WT	TG
LVID; d (mm)	1.59±0.12	2.74±0.36**
LVID; s (mm)	0.58±0.15	2.36±0.38**
LVPW; d (mm)	0.63±0.07	0.49±0.08*
LVPW; s (mm)	1.01±0.13	0.62±0.13**
LVAW; d (mm)	0.69±0.08	0.46±0.07**
LVAW; s (mm)	1.07±0.16	0.60±0.15**
LV Vol; d (μL)	8.4±1.84	20.87±7.45**
LV Vol; s (μL)	0.76±0.57	32.89±11.66**
EF (%)	91.45±5.65	32.89±11.66**
FS (%)	61.43±8.78	15.04±5.74**

a) LVID; d/s, left ventricular diastolic/systolic internal diameter; LVPW, left ventricular posterior wall; LVAW, left ventricular anterior wall; LV Vol; d/s, left ventricular diastolic/systolic volume; EF, ejection fraction; FS, fractional shortening. All values are expressed as mean±SD (n=6–8). *, P<0.05; **, P<0.001 vs. WT.

fibrosis in TG mouse hearts (Figure 4E and F). Similar phenomena were also observed in TG founder mouse 50# (Figure S1C and D in Supporting Information). By electronic microscopy analysis, typically mitochondrial deterioration was found in TG mouse hearts, but not in WT controls (Figure S2A and B in Supporting Information).

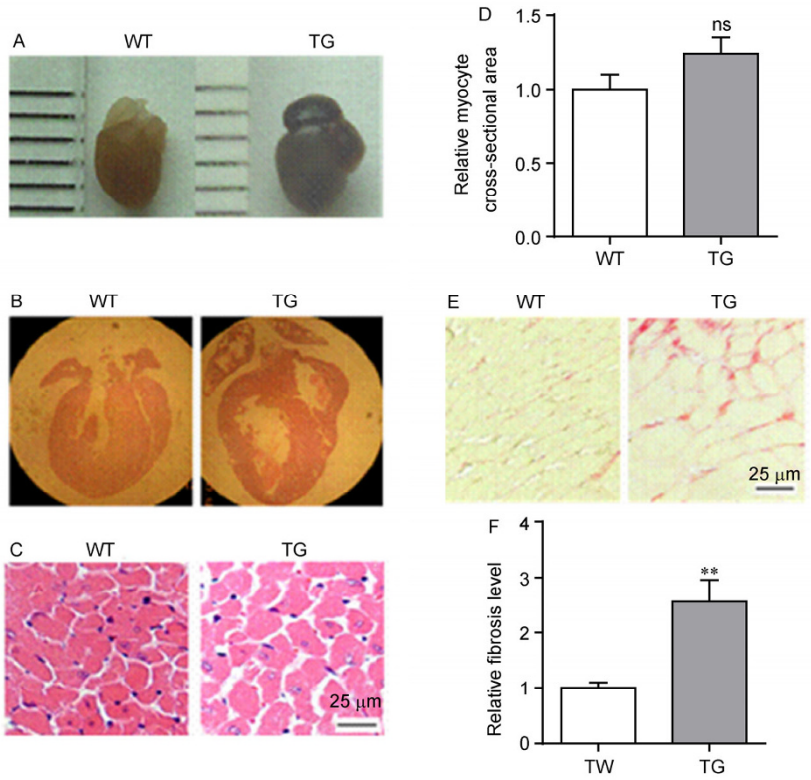

Figure 4 Histological microscopic analysis of SIRT1H363Y TG mice. A, Gross morphology of the hearts from TG mice and WT littermates. B, Microscopic H&E-stained histological section of the hearts. TG mouse hearts were severely dilated in both atria and ventricles compared with those of WT controls. C, H&E from the left ventricles of WT and TG mice for regular histology analysis. D, Relative cross-sectional area in (C) was quantified. ns, no significance. n=5 in each group. E, Picrosirius red staining on histological sections. Fibrosis was present in the ventricles of TG mice. F, The extent of interstitial fibrosis was determined by picrosirus red staining area. Values are expressed as mean±SEM. **, P<0.01 vs. WT.

2.4 Cardiomyocyte apoptosis is enhanced in TG mouse hearts

Studies from our lab and others have provided evidence that SIRT1 can be a cell-survival factor [19,21]. This fact prompted us to investigate whether cardiomyocyte apoptosis was augmented in TG mouse hearts. We used the TUNEL assay to compare apoptosis between TG mouse hearts and those of WT littermates. The heart sections obtained from TG mice exhibited a significantly larger number of TUNEL-positive cardiomyocytes than did controls (Figure 5A and B). Similar findings were also observed in TG founder mouse 50# (Figure S1E in Supporting Information). The level of cleaved caspase-3 was obviously increased in the three lines of TG mouse hearts (Figure 5C). These results indicate that cardiomyocyte apoptosis is enhanced in TG mouse hearts.

2.5 TG mouse hearts show increased p53 acetylation and upregulated bax expression

It has been shown that inhibiting SIRT1 can improve p53 transcriptional activity and p53-dependent apoptosis in cultured cells [3,19]. However, no significant change was observed in total level of p53 protein between TG and WT mouse hearts. Interestingly, the level of p53 acetylation was significantly upregulated in TG mouse hearts (Figure 6A). To assess the consequence of p53 acetylation，Western blot analysis was performed for p53-regulated genes coding proteins, including Bax, Bcl-2, and Bcl-xL. The expression levels for Bax were approximately 2.5-fold higher in TG versus WT mouse hearts. Meanwhile, levels of Bcl-2, Bcl-XL in TG mouse hearts were similar to WT controls (Figure 6B). We further examined key signaling molecules involved in the Bax-mediated apoptosis pathway (upstream of caspase-3 activation) by Western blot. The level of Apaf-1 protein and the cleavage of caspase-9 were significantly up-regulated in TG mouse hearts (Figure 6C), whereas the protein abundance of c-FLIP and caspase-8 was not (Figure S3 in Supporting Information). In addition, *Bax* mRNA was increased approximately 5.5-fold in TG mouse hearts, suggesting the transcriptional activation of this gene (Figure 6D). We further investigated the levels of other p53-regulated proapoptotic target genes, including *Puma* and *Noxa*. We found that the expression level for Puma was significantly enhanced in TG mouse hearts (Figure 6E). Consistent with these results in TG mice, adenoviral expression of SIRT1H363Y significantly upregulated Bax protein in neonatal rat ventricular myocytes, and the level of

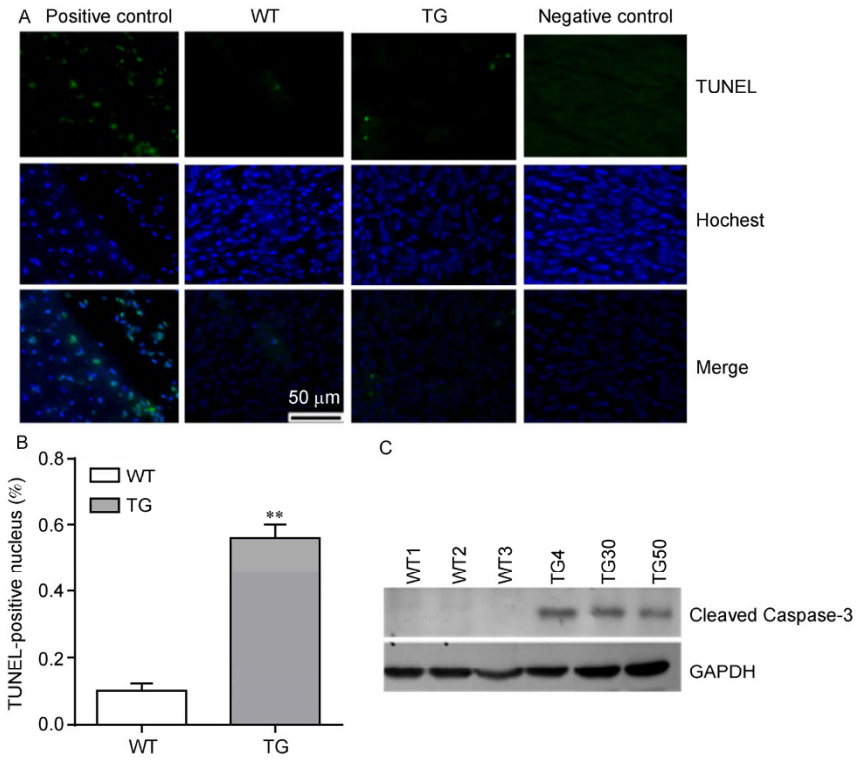

Figure 5 Cardiomyocyte apoptosis is enhanced in TG mouse hearts. A, TUNEL assays from TG mice and WT littermates. Representative TUNEL staining (top), Hoechst staining (middle), and merged image (bottom). Positive and negative controls for the TUNEL assays comprised treatment with DNase I and omission of TdT during the enzymatic reaction, respectively. B, Statistical summary of the assay in (A). Percentage of apoptosis was determined by the number of TUNEL positive myocytes divided by that of Hoechst-positive nuclei. Values are expressed as mean±SEM (n=6). ** , P<0.01 vs. WT. C, Western blot analysis of cleaved caspase-3 expression in the three lines of TG mouse hearts and WT controls. GAPDH was used as loading control.

p53 acetylation was also augmented. Conversely, the Bax protein level and p53 acetylation were reduced with adenoviral SIRT1 overexpression (Figure S4 in Supporting Information). Overall, these data suggest that p53 acetylation and Bax-mediated pathway were involved in apoptosis in TG mouse hearts.

3 Discussion

It has been shown that only a small percentage of *Sirt1*$^{-/-}$ mice survive the first week of life [11], which supports the essential role of SIRT1 but makes it difficult to analyze the function of SIRT1 in the early stage of postnatal hearts. In the present study, we use a strategy to repress the deacetylase activity of SIRT1 in heart by cardiac-specifically overexpressing a dominant negative form of SIRT1. This strategy of repressing SIRT1 activity resulted in a series of phenotypes, including cardiomyocyte apoptosis associated with p53/Bax pathway, early-onset heart failure and premature death, which were not observed in the studies using conventional methods.

We first found that the early postnatal hearts expressed the highest level of SIRT1 deacetylase activity (Figure 1), suggesting that deacetylase activity of SIRT1 is involved in the regulation of cardiac function in the early postnatal hearts. Cardiac specific SIRT1H363Y transgenic mice showed a significant decrease in SIRT1 deacetylase activity and developed dilated cardiomyopathy. Accordingly, most of them died from postnatal days 8 to 12 because of early-onset heart failure (Figure 3A and F). In addition, high-resolution echocardiography allows direct and continuous *in vivo* assessment of cardiac structure and function in the TG mice (Figure 3D and E). These results support the essential roles of SIRT1 deacetylase activity in the early stage of postnatal hearts.

Very recently, Planavila et al. [38] showed that a small percentage of *Sirt1*$^{-/-}$ mice that could survive to adulthood developed dilated cardiomyopathy, which is somewhat similar with the findings in TG founder mouse 50#. Thus, loss of SIRT1 deacetylase activity in the *Sirt1*$^{-/-}$ survivors contributes to dilated cardiomyopathy in late stage of postnatal hearts. Here we used dominant negative form of SIRT1 (SIRT1H363Y) overexpression to inhibit the deacetylase of SIRT1, whereas the study of Planavila et al. used knockout mice expressing a deacetylase-activity absent form of SIRT1 protein [38]. Compared to loss-of-function mutation of SIRT1 protein, dominant negative form of SIRT1 (SIRT1H363Y) protein has potential dominant negative effects on cardiac functions, which may explain the more

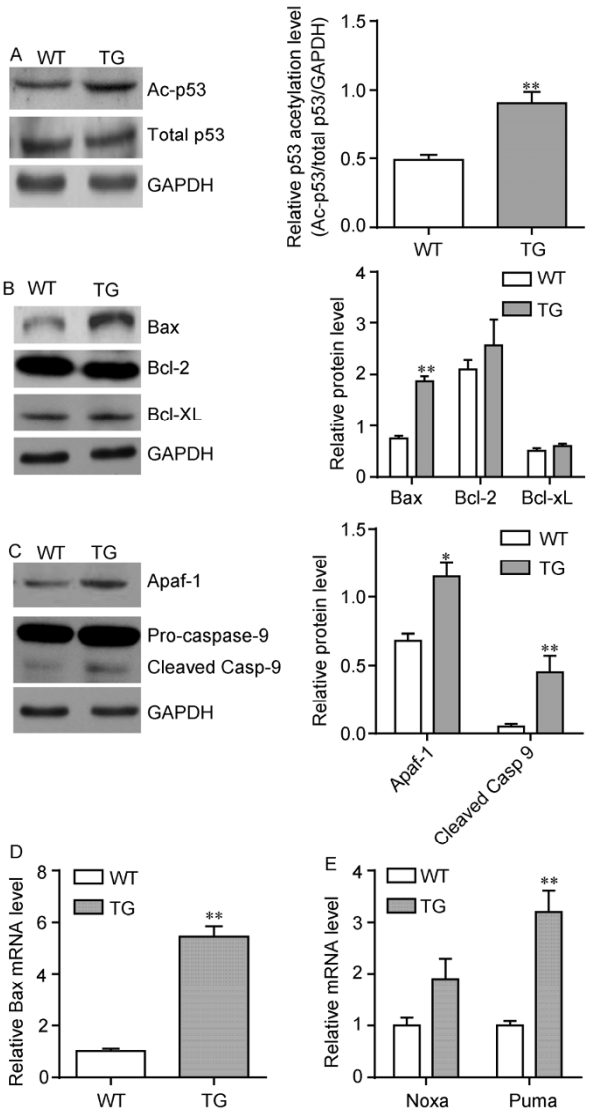

Figure 6 Acetylated p53-Bax-mediated signaling pathway was involved in increased apoptosis in TG mouse hearts. A, Western blot analysis of p53 expression and p53 acetylation (n=6). GAPDH was used as loading control. Left, representative blots; right, quantitative results. **, P<0.01 vs. WT. B, Western blot analysis was performed to determine levels of Bax, Bcl-2 and Bcl-XL (n=6). GAPDH was used as loading control. Left, representative blots; right, quantitative results. **, P<0.01 vs. WT. C, Western blot analysis of important molecules in apoptosis pathways. Apaf-1 and caspase-9, which are important in mitochondria-mediated apoptosis (n=6). GAPDH was used as loading control. Left, representative blots; right, quantitative results. *, P<0.05; **, P<0.01 vs. WT. D, Real-time PCR analysis of Bax mRNA level (n=4). Bax mRNA was normalized to GAPDH mRNA. **, P<0.01 vs. WT. E, Real-time PCR analysis of Noxa and Puma mRNA levels. Noxa and Puma mRNA were normalized to GAPDH mRNA (n=4). **, P<0.01 vs. WT.

severe phenotype of our transgenic mice, including the earlier onset of cardiomyopathy and heart failure.

Cardiomyocyte apoptosis is greatly raised in dilated cardiomyopathy, which is characterized by the gradual development of heart failure [39]. Both the mitochondrial and death receptor-initiated pathways have been shown to activate caspase-3, which is sufficient to induce cardiomyocyte apoptosis and dilated cardiomyopathy [40]. In the previous study, Planavila et al. [38] observed dilated cardiomyopathy and mitochondria dysfunction in SIRT1-deficient mice. They attributed those effects to Mef2, which is crucial both for cardiac differentiation and heart-specific gene expression and also for the control of mitochondrial biogenesis. SIRT1 is a pivotal survival factor for cardiomyocytes under stress [21,22]. However, it remains unclear whether SIRT1 affects cardiomyocyte survival during the early postnatal period. In the present study, we systemically studied whether SIRT1 participates in cardiac function via maintaining cardiomyocyte survival and the underlying mechanism. Our results showed that the cleavage of caspase-9 was significantly increased in TG mouse hearts (Figure 6C), whereas the levels of caspase-8 and its inhibitor c-FLIP were not increased (Figure S3 in Supporting Information). Accordingly, mitochondrial deterioration was found typically in TG mouse hearts (Figure S2A and B in Supporting Information). Thus, a significant increase in activation of caspase-3 and cardiomyocyte apoptosis were observed in TG mouse hearts (Figure 5). Therefore, our data suggest that inhibition of SIRT1 deacetylase activity enhances mitochondria-associated apoptosis in cardiomyocytes and induces the resultant dilated cardiomyopathy and heart failure.

p53 acetylation correlates well with p53-mediated transcriptional activation and is absolutely required for its activation as an indispensable event that enables the p53-mediated stress response [41]. SIRT1 activator resveratrol attenuates doxorubicin-induced cardiomyocyte apoptosis and reduces p53 acetylation [42]. Here we found that acetylation of endogenous p53 was significantly increased with SIRT1H363Y overexpression, and Bax expression was abundant and dramatically upregulated at both the RNA and protein levels in the dilated TG mouse hearts (Figure 6A, B and D). Bax can participate in the mitochondria-mediated apoptosis as an indirect target of p53 through Puma and is also absolutely required for Puma-mediated apoptosis [43]. Thus, the upregulation of Puma may augment Bax-mediated apoptosis as previously reported [44]. Taken together, our data suggest that cardiomyocyte apoptosis induced by inhibition of SIRT1 deacetylase activity is, at least in part, due to increased p53 acetylation and upregulated Bax expression. However, other alternative pathway may exist. A recent report showed that resveratrol, a known SIRT1 activator, mitigates pro-apoptotic signaling in senescent heart through deacetylation mechanism of SIRT1 in repressing Foxo1/Bim-associated pro-apoptotic signaling axis [45]. Additionally, a previous work showed that the effect of SIRT1-TG is dose-dependent [22], thus it remains further to investigate whether this manner exists in our system.

In summary, we demonstrated that dominant negative form of SIRT1H363Y overexpression inhibits of SIRT1 deacetylase activity in mouse heart, and causes cardiomyocyte apoptosis, cardiac dysfunction, early-onset heart failure

and premature death. These findings suggest that SIRT1, the longevity gene, plays important roles not only in retarding age-dependent cardiac dysfunction but also in maintaining cardiomyocyte homeostasis and survival in the early stage of postnatal hearts.

We acknowledge Dr. Liu ZhiPing from University of Texas Southwestern Medical Center for important reading of the manuscript. We are grateful to Prof. Zhang YouYi, Dr. Xiao Han from Peking University Third Hospital for technical assistance with echocardiography. This work was supported by the National Natural Science Foundation of China (31271227, 81161120551) and the National Basic Research Program of China (2011CB503902).

1 Gasser SM, Cockell MM. The molecular biology of the SIR proteins. Gene, 2001, 279: 1–16
2 Frye RA. Characterization of five human cDNAs with homology to the yeast SIR2 gene: Sir2-like proteins (sirtuins) metabolize NAD and may have protein ADP-ribosyltransferase activity. Biochem Biophys Res Commun, 1999, 260: 273–279
3 Luo J, Nikolaev AY, Imai S, Chen D, Su F, Shiloh A, Guarente L, Gu W. Negative control of p53 by Sir2alpha promotes cell survival under stress. Cell, 2001, 107: 137–148
4 Vaziri H, Dessain SK, Ng Eaton E, Imai SI, Frye RA, Pandita TK, Guarente L, Weinberg RA. hSIR2(SIRT1) functions as an NAD-dependent p53 deacetylase, Cell, 2001, 107: 149–159
5 Guarente L, Picard F. Calorie restriction--the SIR2 connection. Cell, 2005, 120: 473–482
6 Guarente L, Franklin H. Epstein Lecture: Sirtuins, aging, and medicine. N Engl J Med, 2011, 364: 2235–2244
7 Haigis MC, Sinclair DA. Mammalian sirtuins: biological insights and disease relevance. Annu Rev Pathol, 2010, 5: 253–295
8 Herranz D, Munoz-Martin M, Canamero M, Mulero F, Martinez-Pastor B, Fernandez-Capetillo O, Serrano M. Sirt1 improves healthy ageing and protects from metabolic syndrome-associated cancer. Nat Commun, 2010, 1: 3
9 Pfluger PT, Herranz D, Velasco-Miguel S, Serrano M, Tschop MH. Sirt1 protects against high-fat diet-induced metabolic damage. Proc Natl Acad Sci USA, 2008, 105: 9793–9798
10 Sakamoto J, Miura T, Shimamoto K, Horio Y. Predominant expression of Sir2alpha, an NAD-dependent histone deacetylase, in the embryonic mouse heart and brain. FEBS Lett, 2004, 556: 281–286
11 Cheng HL, Mostoslavsky R, Saito S, Manis JP, Gu Y, Patel P, Bronson R, Appella E, Alt FW, Chua KF. Developmental defects and p53 hyperacetylation in Sir2 homolog (SIRT1)-deficient mice. Proc Natl Acad Sci USA, 2003, 100: 10794–10799
12 Potente M, Ghaeni L, Baldessari D, Mostoslavsky R, Rossig L, Dequiedt F, Haendeler J, Mione M, Dejana E, Alt FW, Zeiher AM, Dimmeler S. SIRT1 controls endothelial angiogenic functions during vascular growth. Genes Dev, 2007, 21: 2644–2658
13 Wen L, Chen Z, Zhang F, Cui X, Sun W, Geary GG, Wang Y, Johnson DA, Zhu Y, Chien S, Shyy JY. Ca^{2+}/calmodulin-dependent protein kinase kinase beta phosphorylation of Sirtuin 1 in endothelium is atheroprotective. Proc Natl Acad Sci USA, 2013, 110: E2420–E2427
14 Zhang QJ, Wang Z, Chen HZ, Zhou S, Zheng W, Liu G, Wei YS, Cai H, Liu DP, Liang CC. Endothelium-specific overexpression of class III deacetylase SIRT1 decreases atherosclerosis in apolipoprotein E-deficient mice. Cardiovasc Res, 2008, 80: 191–199
15 Gorenne I, Kumar S, Gray K, Figg N, Yu H, Mercer J, Bennett M. Vascular smooth muscle cell sirtuin 1 protects against DNA damage and inhibits atherosclerosis. Circulation, 2013, 127: 386–396
16 Stein S, Lohmann C, Schafer N, Hofmann J, Rohrer L, Besler C, Rothgiesser KM, Becher B, Hottiger MO, Boren J, McBurney MW, Landmesser U, Luscher TF, Matter CM. SIRT1 decreases Lox-1-mediated foam cell formation in atherogenesis. Eur Heart J, 2010, 31: 2301–2309
17 Zhou S, Chen HZ, Wan YZ, Zhang QJ, Wei YS, Huang S, Liu JJ, Lu YB, Zhang ZQ, Yang RF, Zhang R, Cai H, Liu DP, Liang CC. Repression of P66Shc expression by SIRT1 contributes to the prevention of hyperglycemia-induced endothelial dysfunction. Circ Res, 2011, 109: 639–648
18 Li L, Zhang HN, Chen HZ, Gao P, Zhu LH, Li HL, Lv X, Zhang QJ, Zhang R, Wang Z, She ZG, Zhang R, Wei YS, Du GH, Liu DP, Liang CC. SIRT1 acts as a modulator of neointima formation following vascular injury in mice. Circ Res, 2011, 108: 1180–1189
19 Alcendor RR, Kirshenbaum LA, Imai S, Vatner SF, Sadoshima J. Silent information regulator 2alpha, a longevity factor and class III histone deacetylase, is an essential endogenous apoptosis inhibitor in cardiac myocytes. Circ Res, 2004, 95: 971–980
20 Pillai JB, Isbatan A, Imai S, Gupta MP, Poly(ADP-ribose) polymerase-1-dependent cardiac myocyte cell death during heart failure is mediated by NAD+ depletion and reduced Sir2alpha deacetylase activity. J Biol Chem, 2005, 280: 43121–43130
21 Zheng W, Lu YB, Liang ST, Zhang QJ, Xu J, She ZG, Zhang ZQ, Yang RF, Mao BB, Xu Z, Li L, Hao DL, Lu J, Wei YS, Chen HZ, Liu DP. SIRT1 mediates the protective function of Nkx2.5 during stress in cardiomyocytes. Basic Res Cardiol, 2013,108: 364
22 Alcendor RR, Gao S, Zhai P, Zablocki D, Holle E, Yu X, Tian B, Wagner T, Vatner SF, Sadoshima J, Sirt1 regulates aging and resistance to oxidative stress in the heart. Circ Res, 2007, 100: 1512–1521
23 Planavila A, Iglesias R, Giralt M, Villarroya F. Sirt1 acts in association with PPARalpha to protect the heart from hypertrophy, metabolic dysregulation, and inflammation. Cardiovasc Res, 2011, 90: 276–284
24 Oka S, Alcendor R, Zhai P, Park JY, Shao D, Cho J, Yamamoto T, Tian B, Sadoshima J. PPARalpha-Sirt1 complex mediates cardiac hypertrophy and failure through suppression of the ERR transcriptional pathway. Cell Metab, 2011, 14: 598–611
25 Shalwala M, Zhu S-G, Das A, Salloum FN, Xi L, Kukreja RC. Sirtuin 1 (SIRT1) Activation Mediates Sildenafil Induced Delayed Cardioprotection against Ischemia-Reperfusion Injury in Mice. PLoS One, 2014, 9: e86977
26 Rohrbach S, Aslam M, Niemann B, Schulz R. Impact of caloric restriction on myocardial ischemia/reperfusion injury and new therapeutic options to mimic its effects. Br J Pharmacol, 2014, 171: 2964–2992
27 Hsu C-P, Zhai P, Yamamoto T, Maejima Y, Matsushima S, Hariharan N, Shao D, Takagi H, Oka S, Sadoshima J. Silent Information Regulator 1 Protects the Heart From Ischemia/Reperfusion. Circulation, 2010, 122: 2170–2182
28 Mattagajasingh I, Kim CS, Naqvi A, Yamamori T, Hoffman TA, Jung SB, DeRicco J, Kasuno K, Irani K. SIRT1 promotes endothelium-dependent vascular relaxation by activating endothelial nitric oxide synthase. Proc Natl Acad Sci USA, 2007, 104: 14855–14860
29 Zhou S, Chen HZ, Wan YZ, Zhang QJ, Wei YS, Huang S, Liu JJ, Lu YB, Zhang ZQ, Yang RF, Zhang R, Cai H, Liu DP, Liang CC. Repression of P66Shc expression by SIRT1 contributes to the prevention of hyperglycemia-induced endothelial dysfunction. Circ Res, 2011, 109: 639–648
30 Guarani V, Deflorian G, Franco CA, Kruger M, Phng LK, Bentley K, Toussaint L, Dequiedt F, Mostoslavsky R, Schmidt MH, Zimmermann B, Brandes RP, Mione M, Westphal CH, Braun T, Zeiher AM, Gerhardt H, Dimmeler S, Potente M. Acetylation-dependent regulation of endothelial Notch signalling by the SIRT1 deacetylase. Nature, 2011, 473: 234–238
31 Zu Y, Liu L, Lee MY, Xu C, Liang Y, Man RY, Vanhoutte PM, Wang Y. SIRT1 promotes proliferation and prevents senescence through targeting LKB1 in primary porcine aortic endothelial cells. Circ Res, 2010, 106: 1384–1393
32 Barbosa MT, Soares SM, Novak CM, Sinclair D, Levine JA, Aksoy P, Chini EN. The enzyme CD38 (a NAD glycohydrolase, EC 3.2.2.5) is necessary for the development of diet-induced obesity. Faseb J, 2007,

21: 3629–3639
33 Takata T, Ishikawa F. Human Sir2-related protein SIRT1 associates with the bHLH repressors HES1 and HEY2 and is involved in HES1- and HEY2-mediated transcriptional repression. Biochem Biophys Res Commun, 2003, 301: 250–257
34 Gulick J, Subramaniam A, Neumann J, Robbins J. Isolation and characterization of the mouse cardiac myosin heavy chain genes. J Biol Chem, 1991, 266: 9180–9185
35 Chen H, Yong W, Ren S, Shen W, He Y, Cox KA, Zhu W, Li W, Soonpaa M, Payne RM, Franco D, Field LJ, Rosen V, Wang Y, Shou W. Overexpression of bone morphogenetic protein 10 in myocardium disrupts cardiac postnatal hypertrophic growth. J Biol Chem, 2006, 281: 27481–27491
36 Li HL, Zhuo ML, Wang D, Wang AB, Cai H, Sun LH, Yang Q, Huang Y, Wei YS, Liu PP, Liu DP, Liang CC. Targeted cardiac overexpression of A20 improves left ventricular performance and reduces compensatory hypertrophy after myocardial infarction. Circulation, 2007, 115: 1885–1894
37 Zhang QJ, Chen HZ, Wang L, Liu DP, Hill JA, Liu ZP. The histone trimethyllysine demethylase JMJD2A promotes cardiac hypertrophy in response to hypertrophic stimuli in mice. J Clin Invest, 2011, 121: 2447–2456
38 Planavila A, Dominguez E, Navarro M, Vinciguerra M, Iglesias R, Giralt M, Lope-Piedrafita S, Ruberte J, Villarroya F. Dilated cardiomyopathy and mitochondrial dysfunction in Sirt1-deficient mice: a role for Sirt1-Mef2 in adult heart. J Mol Cell Cardiol, 2012, 53: 521–531
39 Narula J, Haider N, Virmani R, DiSalvo TG, Kolodgie FD, Hajjar RJ, Schmidt U, Semigran MJ, Dec GW, Khaw BA. Apoptosis in myocytes in end-stage heart failure. N Engl J Med, 1996, 335: 1182–1189
40 Wencker D, Chandra M, Nguyen K, Miao W, Garantziotis S, Factor SM, Shirani J, Armstrong RC, Kitsis RN. A mechanistic role for cardiac myocyte apoptosis in heart failure. J Clin Invest, 2003, 111: 1497–1504
41 Tang Y, Zhao W, Chen Y, Zhao Y, Gu W. Acetylation is indispensable for p53 activation. Cell, 2008, 133: 612–626
42 Zhang C, Feng Y, Qu S, Wei X, Zhu H, Luo Q, Liu M, Chen G, Xiao X. Resveratrol attenuates doxorubicin-induced cardiomyocyte apoptosis in mice through SIRT1-mediated deacetylation of p53. Cardiovasc Res, 2011, 90: 538–545
43 Nakano K, Vousden KH. PUMA, a novel proapoptotic gene, is induced by p53. Mol Cell, 2001, 7: 683–694
44 Luo X, He Q, Huang Y, Sheikh MS. Transcriptional upregulation of PUMA modulates endoplasmic reticulum calcium pool depletion-induced apoptosis via Bax activation. Cell Death Differ, 2005, 12: 1310–1318
45 Sin TK, Yu AP, Yung BY, Yip SP, Chan LW, Wong CS, Ying M, Rudd JA, Siu PM. Modulating effect of SIRT1 activation induced by resveratrol on Foxo1-associated apoptotic signalling in senescent heart. J Physiol, 2014, doi:10.1113/jphysiol.2014.271387

Supporting Information

Figure S1 Phenotypic and histological microscopic analysis of TG founder mouse 50#. A, Gross morphology of the heart from TG founder mouse 50# and WT littermates. Both atria and ventricles of TG founder mouse 50# displayed substantial dilation with a large organized thrombus in the left atrium. B, Tissue weight to body weight ratios for TG founder mouse 50# and WT littermates. Hearts and lungs were harvested to identify mice that had signs of pulmonary edema, an indication of heart failure. The heart failure phenotype of TG founder mouse 50# was determined retrospectively and was based on the criterion of wet lung weight to body weight ratio. C, H&E from the left ventricles of TG founder mouse 50# and WT littermates for regular histology analysis. Scale bar: 50μm. D, The extent of interstitial fibrosis determined by picrosirus red staining area. Quantitative assessment of the fibrotic area of the myocardium was performed in five randomly selected fields by quantitative morphometry of left ventricular tissue sections. E, Statistical summary of TUNEL assays from TG founder mouse 50# and WT littermates. Values are mean±SEM. **, $P<0.01$.

Figure S2 Electron microscopic view of the ventricles of WT and TG mice. The tissue samples of the left ventricular free wall were preserved immediately after animal sacrifice and processed as previously described [1]. For electron microscopy, left ventricular walls from 7-day-old mice were fixed in 2.5% glutaraldehyde and 100 mmol L^{-1} calcium cacodylate overnight, and subsequently postfixed with 1% OsO4; stained en bloc with 2% uranyl acetate; embedded in Apon 812; sectioned; and stained with 4% uranyl acetate/Reynold's lead citrate. The sections were examined using a JEOL TEM-1010 electron microscope (JEOL, Tokyo, Japan). By electronic microscopy analysis, mitochondrial deterioration typically was found in TG mouse hearts in B, but not in WT controls in A. Scale bar, 200 nm.

Figure S3 Western blot analysis of c-FLIP and caspase-8 expression, which participate in death-receptor mediated apoptosis (n=6). GAPDH was used as loading control. Top, Representative blots; Bottom, quantitative results. All values are expressed as mean±SEM.

Figure S4 Western blot analysis of Bax expression and p53 acetylation in neonatal rat ventricular myocytes. To overexpress hSIRT1 and hSIRT1H363Y in the cardiomyocytes, an adenovirus vector expressing hSIRT1 (Ad-hSIRT1) and an adenovirus vector expressing hSIRT1H363Y (Ad-hSIRT1H363Y) were constructed. Packaging and amplification of adenoviral vectors were performed as previously described [2]. Adenoviral-Green Fluorescence Protein (Ad-GFP) was used as a control. Experiments were performed at a multiplicity of infection of 100 plaque-forming units/cell. Cardiomyocytes were infected with Ad-hSIRT1, control Ad-GFP or Ad-hSIRT1H363Y and Western blot analysis were performed on lysates collected 40 h after virus washout and starvation. β-Actin was used as loading control. Each assay was done in triplicate.

Table S1 Primers for conventional reverse transcription PCR or real-time PCR

The supporting information is available online at life.scichina.com and link.springer.com. The supporting materials are published as submitted, without typesetting or editing. The responsibility for scientific accuracy and content remains entirely with the authors.